Fabrication and Properties of Irradiation-Cross-Linked Poly(vinyl alcohol)/Clay Aerogel Composites

Hong-Bing Chen,*[†] Bo Liu,[†] Wei Huang,[†] Jun-Sheng Wang,[§] Guang Zeng,[†] Wen-Hao Wu,[†] and David A. Schiraldi*[‡]

[†]Institute of Nuclear Physics and Chemistry, Chinese Academy of Engineering Physics, Mianyang, Sichuan 621000, China

[‡]Department of Macromolecular Science & Engineering, Case Western Reserve University, Cleveland, Ohio 44106-7202, United States

[§]Tianjin Fire Research Institute of the Ministry of Public Security, Tianjin 300381, China

ABSTRACT: Poly(vinyl alcohol) (PVOH)/clay aerogel composites were fabricated by an environmentally friendly freeze-drying of the aqueous precursor suspensions, followed by cross-linking induced by gamma irradiation without chemical additives. The influences of cross-linking conditions, *i.e.*, absorbed dose and polymer loading as well as density on the aerogel structure and properties, were investigated. The absorbed dose of 30 kGy was found to be the optimum dose for fabricating strong PVOH composites; the compressive modulus of an aerogel prepared from an aqueous suspension containing 2 wt % PVOH/8 wt % clay increased 10-fold, and that containing 1 wt % PVOH/9 wt % clay increased 12 times upon cross-linking with a dose of 30 kGy. Increasing the solids concentration led to an increase in the mechanical strength, in accordance with the changes in microstructure from layered structure to network structure. The increase of absorbed dose also led to decreased porous size of the network structure. Cross-linking and the increase of the PVOH lead to decreased thermal stability. The strengthened PVOH/clay aerogels possess very low flammability, as measured by cone calorimetry, with heat, smoke, and volatile products release value decreasing as increasing clay content. The mechanism of flame retardation in these materials was investigated with weight loss, FTIR, WAXD, and SEM of the burned residues. The proposed mechanism is that with decreasing fuel content (increasing clay content), increased heat and mass transport barriers are developed; simultaneously low levels of thermal conductivity are maintained during the burning.

KEYWORDS: *aerogel, poly(vinyl alcohol), gamma irradiation, mechanical properties*
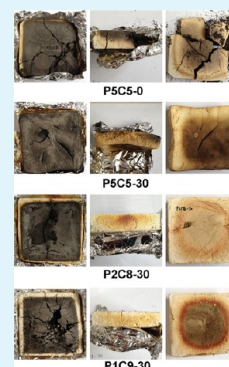
1. INTRODUCTION

Mackenzie and Call first reported montmorillonite clay aerogels prepared using a freeze-drying method in 1950s.[1,2] The fibrous montmorillonite structures obtained in this manner possessed insufficient mechanical integrity for practical use. Van Olphen investigated that the layers within clay aerogels are linked edge-to-face much like a "house of cards", due to opposite surface and edge charges that exist in clays.[3] The porous clay microstructure of these materials results from the grain boundries of ice crystals produced during freezing, in which the ice crystals grow and push clay particles aside to promote parallel platelet alignment. Nakazawa et al. revealed that the decrease in clay concentration and freezing rates results in the morphological structure change from polygonal cells to thin layers.[4-6] At low concentrations of clay, the suspension viscosities present little resistance to the growth of an ice front, allowing for the formation of lamellar ice layers. For high-viscosity solutions, growth of ice crystals is retarded by the fluid viscosity, resulting in more fractal growth and secondary crystallization of water and the generation of a greater number of structural links between the aerogel layers. The lower freezing rate allows the generation of large and fine ice crystals, which is similar to that in low solution concentration. Poly(vinyl alcohol) (PVOH) is a highly hydrophilic and

water-soluble polymer[7] and easily transforms to a hydrogel through different techniques, such as freeze−thaw inducement of crystallization,[8-15] acid-catalyzed dehydration,[16] radical production,[17,18] and chemical cross-linking (diacid, aldehyde, and alkoxysilanes).[19-23] Accordingly, PVOH hydrogels are widely used in drug delivery,[24] contact lenses,[25] wound bandages,[26] dressing tissue engineering,[27] and cell immobilization,[28] due to its low toxicity, high water content, good mechanical properties, and biocompatibility. Cross-linking methods generally require long treatment times or harsh reaction conditions, limiting their use.

PVOH is also used to strengthen clay aerogels through solution blending.[29] The mechanical properties of these aerogels show power law dependence on aerogel density (mainly based upon polymer loading). The mechanically robust, foam-like composites have the potential to be used in packaging, insulation, and absorbent fields.[30] PVOH is however a flammable polymer with a limiting oxygen index (LOI) of 19.7,[31,32] which can require a low PVOH loading in PVOH/

clay aerogels to address fire safety, in conflict with optimized mechanical properties.

Cross-linking methods are an effective means of increasing aerogel mechanical properties. Pojanavaraphan et al.[33] prepared cross-linked natural rubber clay aerogel composites through a solution process using sulfur monochloride as the active agent; the mechanical properties increased 26-fold compared to control materials. In our previous studies, a facile fabrication of poly(vinyl alcohol) gels and derivative aerogels were reported, using water as solvent and divinylsulfone as cross-linking agent, resulting in significantly enhanced mechanical properties. The compressive modulus of aerogel containing 2 wt % PVOH/8 wt % clay (density: 0.1 g/cm^3) increased 29-fold upon cross-linking, for example.[34] Chemical cross-linking methods bring unavoidable drawbacks; obtaining homogeneous blends of cross-linking agent and polymer/clay suspension in high viscosity systems is difficult, resulting in low preparation efficiencies and potentially residual unreacted cross-linking agents. Irradiation-induced cross-linking could offer an attractive alternative method for the enhancement of aerogel properties and fabrication efficiency. In the present study we report the production of strengthened PVOH/clay aerogels without use of chemical additives. The cross-linking reaction of PVOH/clay suspension was induced by gamma irradiation, and then the resulting hydrogel materials were converted into PVOH/clay aerogels, via a freeze-drying method. By use of this chemical-free cross-linking process, aerogels possessing high mechanical properties, yet containing the relatively low PVOH contents ideal for reduced flammability could be produced. The morphologies, mechanical properties, combustion behaviors, the mechanisms by which flammability is reduced and their relationships of low polymer loading PVOH/clay aerogel are reported herein for the first time, to the best of our knowledge.

2. EXPERIMENTAL SECTION

2.1. Materials. Poly(vinyl alcohol) (PVOH, Mw 31,000–50,000, 99% hydrolyzed) was purchased from Sigma-Aldrich. Sodium montmorillonite (Na^+-MMT; PGW grade with a cation exchange capacity of 145 mequiv/100 g) was supplied by Nanocor Inc. Deionized (DI) water was prepared using a Purelab flex 3 unit. All reagents were used without further purification.

2.2. Hydrogel and Aerogel Preparation. Percentages of PVOH and clay structural components are given as a percentage of DI water. To produce an aerogel containing 5 wt % PVOH and 5 wt % clay for example (noted as P5C5, where P stands for PVOH, C stands for clay), 5 g of PVOH solid was dissolved in 50 mL of DI water at 80 °C overnight by stirring. Five g of Na^+-MMT was blended with 50 mL of DI water at high speed (20,000 rpm) to create clay suspension. The resulting mixture of clay suspension and PVOH solution were poured into polyethylene vials (diameter: 20 mm; height: 45 mm) and aluminum mold (100 mm × 100 mm × 25 mm) and then irradiated using a ^{60}Co source at the Institute of Nuclear Physics and Chemistry, and the dose rate was 170 Gy/min; note, the vials did not influence the irradiation of samples. The P5C5 with required absorbed doses of 0, 10, 30, 50, and 100 kGy are coded as P5C5-0, P5C5-10, P5C5-30, P5C5-50, and P5C5-100, respectively. Then the resulting hydrogels and the control were frozen in a liquid nitrogen bath (~−196 °C). The frozen samples were dried in a Beijing Sihuan LGJ-25C freeze-dryer with a shelf temperature of 30 °C, where a high vacuum (1–5 Pa) was applied to sublime the ice. The freeze-dry process typically was given 3–4 days to ensure complete drying.

2.3. Characterization. Densities of the aerogel samples were calculated by measuring the mass and dimensions using an analytical balance and a digital caliper. Compression testing was conducted on the cylindrical specimens (~20 mm in diameter and height), using an SANS CMT7000 testing machine, fitted with a 10 kN load cell, at a

crosshead of 10 mm/min. Five samples for each composition were tested for reproducibility. The initial compressive modulus was calculated from the slope of the linear portion of the stress–strain curve. The morphological microstructure of the aerogels and the burned residue were characterized with a ZEISS EVO 18 special edition scanning electron microscope at an acceleration voltage of 10 kV. The samples were prepared by fracturing in liquid nitrogen and then sputter-coated with a thin layer of gold before testing. The thermal stabilities (by thermogravimetric analysis, TGA) were measured on a STA449C apparatus under a nitrogen flow (40 mL/min). About 3 mg of samples was placed in a platinum pan and heated from ambient temperature to 650 °C at a rate of 10 °C/min. The combustion behaviors of cross-linked PVOH/clay aerogel and the control were tested with an FTT cone calorimeter. Specimens with a size of 100 mm × 100 mm × 25 mm were tested under a heat flux of 50 kW/m^2. The heat, smoke, and volatile products release information were recorded. The temperature of the sample bottom was also recorded to evaluate the insulation property of aerogel. The residues of the burned samples are marked as P5C5-0b, P5C5-30b, P2C8-30b, and P1C9-30b, respectively. The FTIR spectra of the burned residue from different positions of sample were carried out with a Nicolet 6700 FTIR spectrometer. Wide-angle X-ray diffraction (WAXD) measurements of MMT clay, aerogel, and the burned residue were performed using an X-ray diffraction in a 2θ range from 2° to 45°.

3. RESULTS AND DISCUSSION

Preparation and Properties of Irradiation-Induced Cross-Linked PVOH/Clay Aerogels. Irradiation-induced cross-linking of polymer solutions are commonly used to fabricate hydrogels, such as those of PEO, starch, and PVP.[35−38] PVOH hydrogels prepared via irradiation have also been reported,[26,27] requiring no use of chemical cross-linking agents. All the samples containing clay and PVOH in this study were demonstrated to generate aerogels with stable, workable structures after cross-linking and freeze-drying (Figure 1),
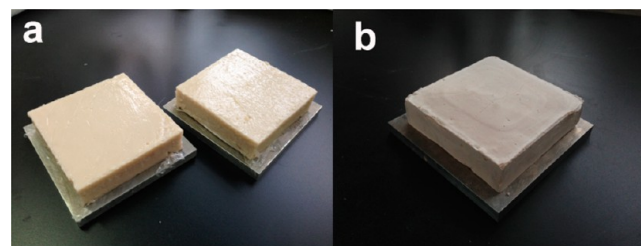

Figure 1. Gamma irradiation-induced P5C5-30 hydrogel composites (a) and the derivative aerogel (b).

whereas cracks or shrinkage occurred in neat PVOH (P10) upon irradiating; clay clearly stabilizes the cross-linked aerogel structures (and in fact stabilizes the samples prior to irradiation, as can be seen with the specific modulus of the polymer-only aerogel; clay and/or irradiation strengthens the structure). The degree of mold shrinkage obtained for the sample excluding clay was considerably greater than those containing clay, as well. The aerogels containing high Na^+-MMT loadings, P5C5, P2C8, and P1C9, exhibited very low levels of shrinkage during the freeze-drying process, with a typical diameter of 18.5–19.0 mm, compared to 20.0 mm of the diameter of vial mold.

The compressive stress–strain curves of the P5C5 with different absorbed doses are shown in Figure 2. The majority of stress–strain curves followed the basic form of classical rigid porous foam behavior, which is a linear elastic deformation at low strain, followed by a densification region beyond the yield point.[39,40] The stress–strain behaviors of the aerogels do not
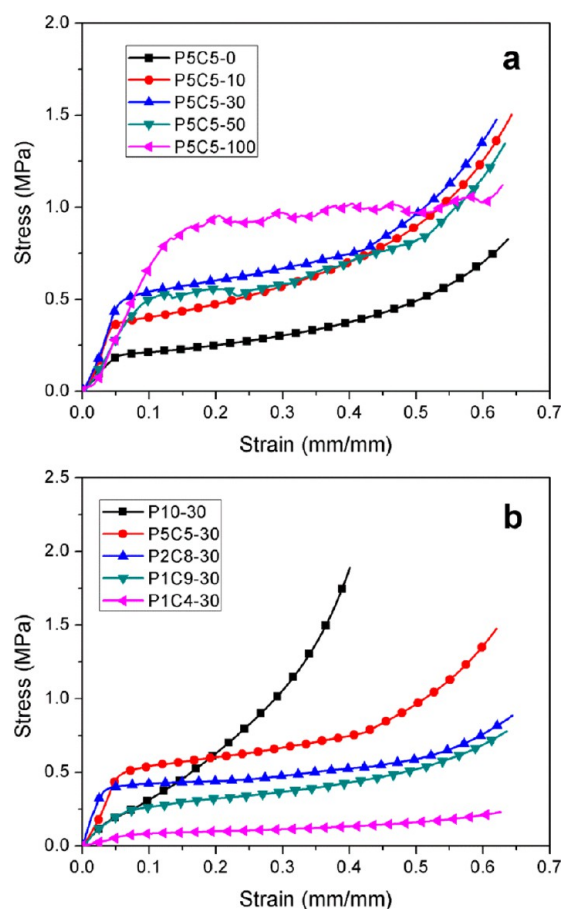
Figure 2. Example strain–stress curves of PVOH/clay aerogels.

significantly with decreasing polymer content. The compressive moduli decrease from 4.56 MPa of P5C5-0 to 0.41 MPa of P1C9-0, the latter lacking usable mechanical properties. Irradiation-induced cross-linking was utilized to strengthen the aerogels, enlarging the workable concentrations in which polymer content could be low enough for better fire-resistance. Accordingly, the morphological structure changes from network to layered structures for the clay-containing samples, as shown in Figure 3. The aerogels show denser structures after irradiation, with the exception of P1C4-30, which contains very low levels of solids. In our previous study,[6,41] it was found that the morphological structure changes from layered structure to network structure with increasing solution viscosity. At high solution viscosities, the aerogel materials tend to be porous with small cell sizes. In this study, liquid nitrogen was used to freeze the samples instead of a solid carbon dioxide/ethanol bath, in which the higher degree of supercooling leads to higher density of nucleates, generating network structure of the resulting aerogels even for the control sample.[3] Both increasing the concentration of polymer/clay in water or cross-linking the polymer are the effective ways to increase the suspension viscosity. Thus, the microstructure of the aerogels changes from a layered to network structure after being cross-linked; cross-linking in turn leads to greater structural integrity, leading to enhanced mechanical properties, as we have previously reported.[6,41]

The compressive moduli of the cross-linked material first increases and then decreases with increasing absorbed doses of radiation. The compressive moduli of P5C5 increase from 4.56 MPa of control, to 9.41 MPa of P5C5-10, then to 11.43 MPa of P5C5-30; it then decreases to approximately 9 MPa for P5C5-50 and P5C5-100. Thirty kGy appears to be optimal for the majority of the samples, representing a balance between radical-induced cross-linking and overall radiation-induced material degradation. At high absorbed doses, radiolysis becomes the main effect, leading to the decrease of compressive moduli. Another possible reason for the decreased mechanical property is the decreased elasticity with increased absorbed dose. The morphological microstructures of P5C5 with different absorbed doses are shown in Figure 4. For the control sample without irradiation, a network structure with irregular pores is evident from the SEM images; pore sizes of approximately 10 μm are

change appreciably with increasing absorbed dose but lose their ductility. The detailed density, compressive modulus, and specific modulus for irradiation induced strengthened PVOH/clay aerogel composites and the control sample are presented in Table 1. For the control samples, neat PVOH (P10) shows good mechanical properties due to the high density for the shrinkable dimension; however, the specific modulus is lower than the majority of aerogel samples containing clay. The mechanical properties of polymer/clay aerogels decrease

Table 1. Mechanical Properties of PVOH/Clay Aerogels[a]

sample	property	P10	P5C5	P2C8	P1C9	P1C4
control	modulus	4.40 ± 1.40	4.56 ± 1.10	1.38 ± 0.22	0.41 ± 0.24	0.06 ± 0.01
	density	0.229 ± 0.010	0.093 ± 0.003	0.084 ± 0.006	0.091 ± 0.002	0.045 ± 0.003
	M/d	19.26 ± 6.46	49.04 ± 13.02	16.27 ± 1.93	4.44 ± 2.51	1.33 ± 0.25
10 kGy	modulus	9.21 ± 1.88	9.41 ± 0.32	3.67 ± 1.14	1.15 ± 0.19	0.095 ± 0.071
	density	0.128 ± 0.005	0.085 ± 0.002	0.084 ± 0.002	0.083 ± 0.002	0.043 ± 0.006
	M/d	71.93 ± 12.37	111.86 ± 4.91	43.65 ± 13.57	13.80 ± 2.15	1.37 ± 0.79
30 kGy	modulus	15.20 ± 1.39	11.43 ± 0.13	13.18 ± 1.26	4.92 ± 3.01	1.26 ± 0.24
	density	0.148 ± 0.013	0.086 ± 0.004	0.083 ± 0.002	0.083 ± 0.001	0.043 ± 0.001
	M/d	102.92 ± 0.24	133.22 ± 4.94	159.36 ± 13.27	59.25 ± 36.07	29.46 ± 4.86
50 kGy	modulus	4.01 ± 0.49	8.99 ± 2.51	4.54 ± 2.26	9.46 ± 3.44	0.97 ± 0.09
	density	0.138 ± 0.006	0.086 ± 0.001	0.083 ± 0.002	0.083 ± 0.002	0.043 ± 0.001
	M/d	29.07 ± 3.42	103.91 ± 27.46	54.61 ± 27.38	102.72 ± 62.77	22.77 ± 2.48
100 kGy	modulus	5.20 ± 0.38	9.30 ± 0	4.46 ± 1.58	4.53 ± 0.60	1.14 ± 0.61
	density	0.138 ± 0.015	0.093 ± 0.002	0.084 ± 0.002	0.080 ± 0.001	0.043 ± 0
	M/d	38.21 ± 5.21	99.54 ± 2.44	53.31 ± 20.09	56.35 ± 7.25	33.53 ± 13.93

[a]Moduli in MPa, densities in g/cm^3, specific moduli (M/d) in MPa-cm^3/g.

Figure 3. SEM micrographs of PVOH/clay aerogels.

Figure 4. SEM micrographs of P5C5 aerogels with various absorbed doses.
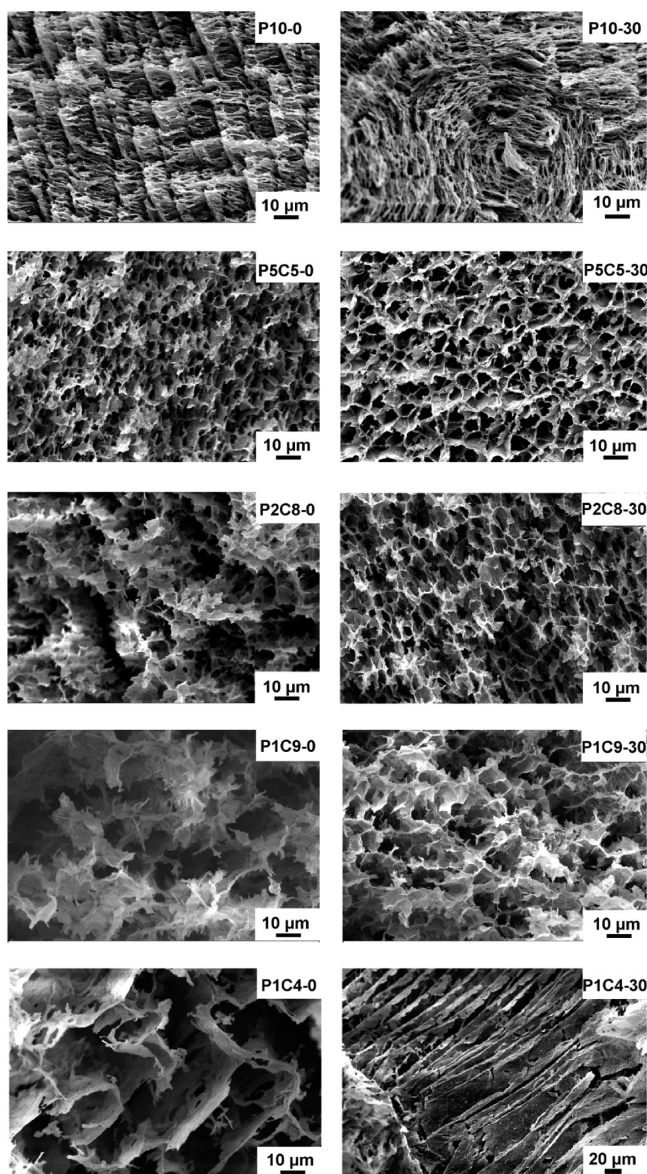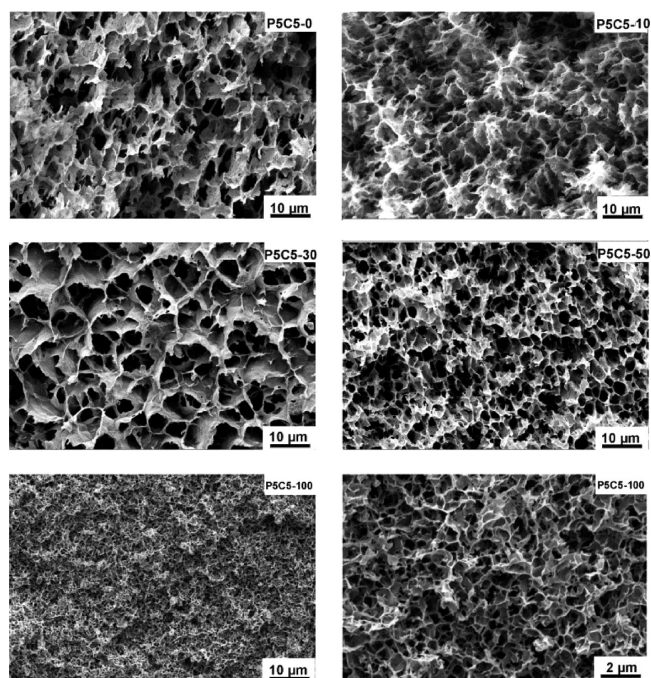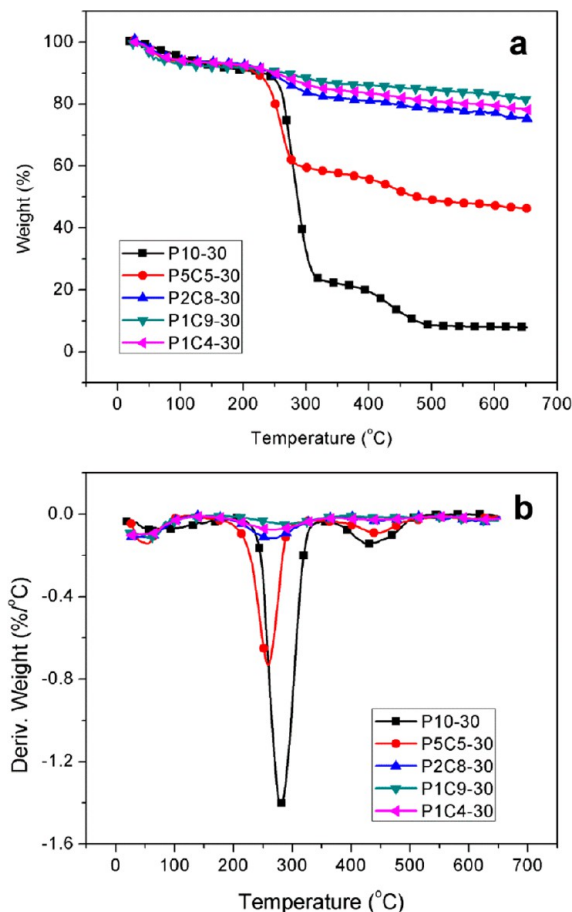

Figure 5. TGA weight loss and DTG curves of strengthened PVOH/clay aerogels.

evident for the composites samples dosed with 10 kGy; for the samples dosed with 30 kGy, more regular structures with pore sizes of 5 to 10 μm were evident. As the absorbed dose was increased to 50 kGy, the resulting aerogels exhibited significantly decreased pore sizes, down to about 2−5 μm; at 100 kGy, pores 1 μm or less were observed. The degree of cross-linking is known to increase with increasing absorbed,[42] leading to decreased pore sizes in the aerogels, quite likely due to restricted chain mobility and therefore difficulty in accommodating the ice fronts which grow during freeze-drying.

Thermal Stability. The thermal stabilities of strengthened PVOH/clay aerogels and the control sample were investigated by TGA, Figures 5 and 6, and Table 2. Both PVOH and clay easily absorb water due to the existence of abundant hydroxyl groups and ionic character. Thus, the first weight loss stage is caused by the desorption of water, $T_{d\,5\%}$, which decreased with increasing clay content. The absorbed dose of γ radiation did not have an obvious impact upon the first weight loss stage. The second weight loss step is observed to begin at about 190 °C, $T_{d\,10\%}$, which is associated with the decomposition of

PVOH (onset decomposition temperature). The cross-linking of polymeric materials usually contributes to their thermal
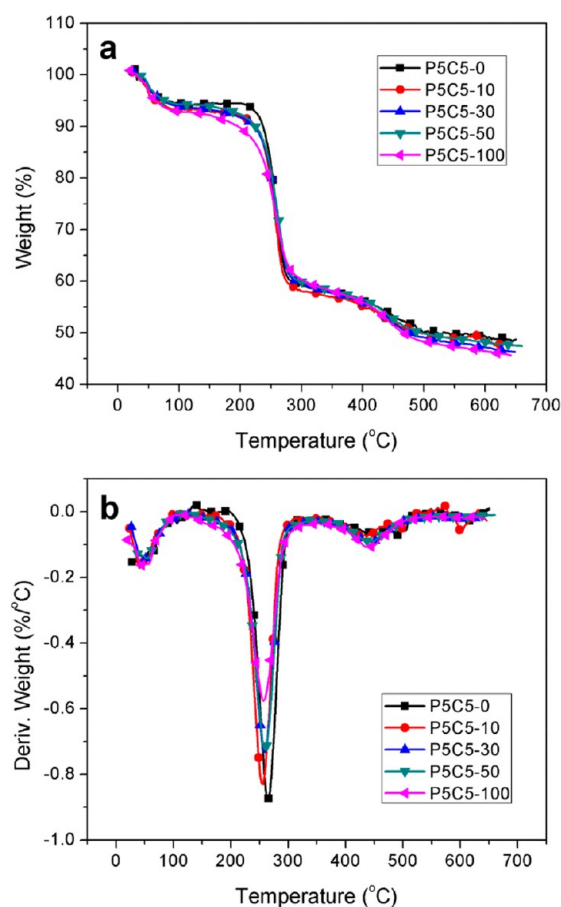
Figure 6. TGA weight loss and DTG curves of P5C5 aerogels with various absorbed dose.

Table 2. TGA Data of Freeze Dried PVOH/Clay Aerogels

samples	$T_{d\ 5\%}$ (°C)	$T_{d\ 10\%}$ (°C)	$T_{d\ max}$ (°C)	dW/dT (%/°C)	residue (%)
P10-30	104.0	201.5	279.0	1.41	7.8
P5C5-0	82.0	243.4	264.0	0.87	48.7
P5C5-10	72.0	223.5	256.0	0.83	47.7
P5C5-30	71.0	221.0	258.9	0.73	46.3
P5C5-50	75.1	217.6	260.1	0.73	47.4
P5C5-100	69.6	194.6	257.1	0.58	45.7
P2C8-30	77.1	245.0	269.5	0.12	75.3
P1C9-30	55.0	267.1	292.1	0.051	81.5
P1C4-30	78.1	250.6	270.0	0.075	78.2

stability;[6,41,43,44] however, the onset decomposition temperatures of the cross-linked PVOH/clay aerogels decreased monotonically with increasing absorbed gamma irradiation doses, probably the result of PVOH radiolysis. It is interesting

to note that the maximum decomposition temperature did not change significantly with increasing absorbed radiation; however, the maximum weight loss rate decreased with increasing dose, most likely due to the decreased chain mobility of photo-cross-linked materials. The final residue weights were not influenced by the degree of irradiation. The gamma irradiation overall had a minor effect upon the thermal stability of these materials, whereas increasing levels of clay (relative to polymer) did increase their stabilities.

Combustion Behavior. The combustion behavior of cross-linked PVOH/clay aerogels and control samples was studied using cone calorimetry, which is widely used to predict the combustion behavior of materials under actual fire conditions. The relevant data of PVOH/clay aerogels, such as time to ignition (TTI), peak of heat release rate (PHRR), mean PHRR, total heat release (THR), time to peak of heat release rate (TTPHRR), total smoke release (TSR), mean specific extinction area (mean SEA), and fire growth rate (FIGRA, can be used to evaluate their flammability), are summarized in Table 3.

TTI, the time required to ignite the sample during cone calorimeter tests, is thought to correlate with combustible gas products from degraded polymer reaching a critical concentration.[45] In this study, P5C5-0, P5C5-30, and P2C8-30 exhibited very short TTI values, less than 5 s. The addition of silicates leads to decreased TTI in most cases, probably due to the catalysis effect of clay to the decomposition of polymer, and the rapid temperature increase on the surface of nanocomposites.[46] For the P1C9-30 material, however, no open fire was observed throughout the entire testing period under 50 kW/m² of heat flux, indicating an extremely low fire risk (also reflecting the low levels of combustible gases present). Figure 7 shows the heat release rate (HRR) of strengthened PVOH/clay aerogels and the control. P5C5-0, P5C5-30, and P2C8-30 burned rapidly after being ignited, with the peak of heat release rate of 140.1, 137, and 73.8 kW/m², respectively. The HRR then decreased to extremely low values with further increasing clay content. It is noted that the HRR of the cross-linked sample (P5C5-30) decreased compared with the control sample (P5C5-0), probably because of the decreased chain mobility and increased difficulty in decomposing the network chain structure to combustible gas products. It is obvious that the only fuel in the aerogel is PVOH, thus the heat release depends on the proportion of PVOH. When the PVOH content further decreases to 10% (P1C9-30), the sample did not appear to ignite with very low PHRR of 10.7 kW/m². The corresponding mean HRR values are 28.3, 24.1, 4.12, and 0 kW/m² for P5C5-0, P5C5-30, P2C8-30, and P1C9-30, respectively.

The THR of P5C5-0, P5C5-30, P2C8-30, and P1C9-30 are 18.5, 16.3, 2.5, and 0.26 MJ/m², respectively (Figure 8). The

Table 3. Burning Parameters of PVOH/Clay Aerogels[a]

sample	TTI (s)	PHRR (kW/m²)	mean HRR (kW/m²)	TTPHRR (s)	THR (MJ/m²)	FIGRA (W/s)	TSR (m²/m²)	mean SEA (m²/kg)	residue (%)
P5C5-0	4	140.1	28.3	15	18.5	9.3	139.6	112.6	78.7
P5C5-30	5	137.1	24.1	20	16.3	6.9	182.3	113.4	76.4
P2C8-30	2	73.8	4.12	15	2.5	4.9	25.5	33.3	90.5
P1C9-30	no flame	10.7	0	15	0.26	0.7	15.0	25.4	94.1

[a]TTI = time to ignition; PHRR = peak heat release rate; HRR = heat release rate; TTPHRR = time to peak heat release; THR = total heat released; FIGRA = fire growth rate; TSR = total smoke released; SEA = specific extinction area.

16231

dx.doi.org/10.1021/am504418w | ACS Appl. Mater. Interfaces 2014, 6, 16227−16236
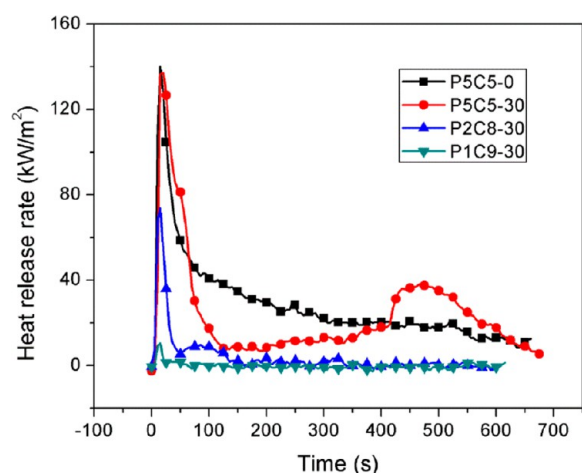
Figure 7. Heat release rate of PVOH/clay aerogel as a function of burning time.

Figure 8. Total heat release of PVOH/clay aerogel as a function of burning time.

Figure 9. Photos of PVOH/clay aerogel residues after burning in cone calorimeter; left top, right bottom.
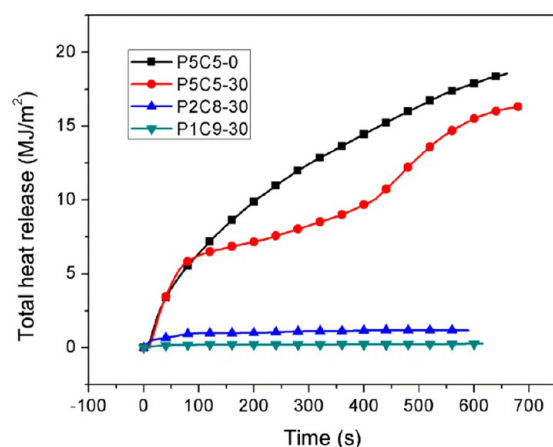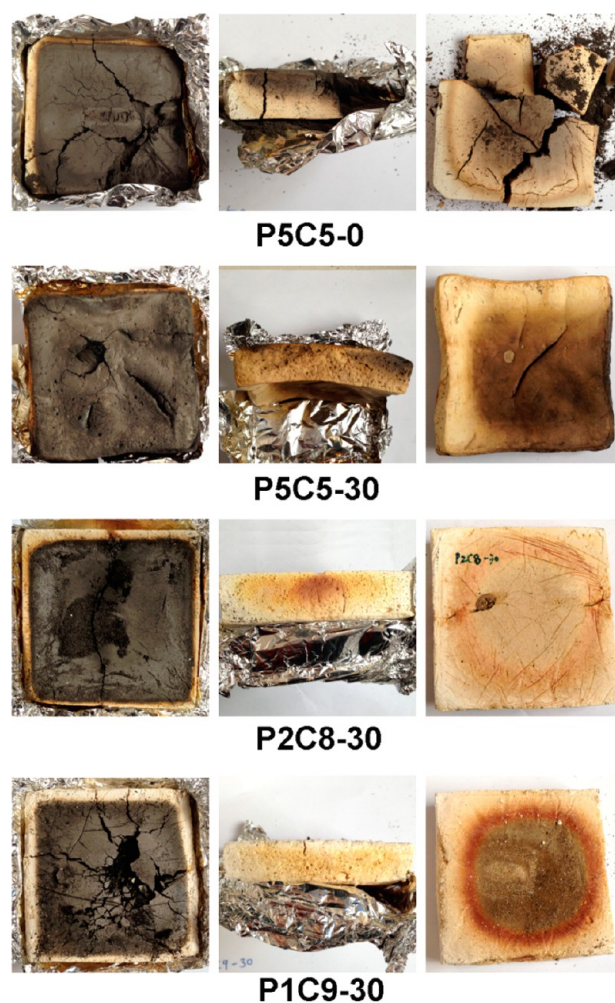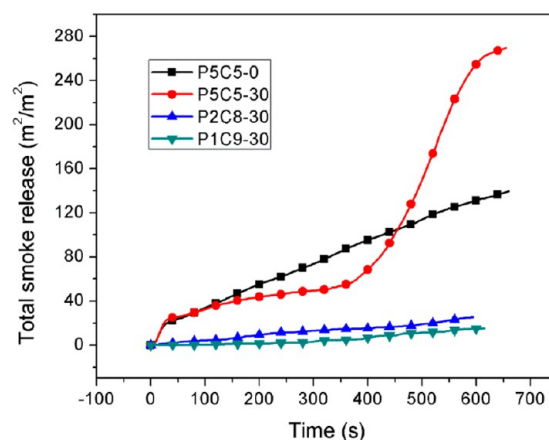

Figure 10. Total smoke release of PVOH/clay aerogel as a function of burning time.

heat release of aerogels is attributed to the PVOH according to the aforementioned discussion. However, the THR is not proportional to the PVOH content, indicating the incomplete combustion of aerogel sample. In fact, the underneath of the cone calorimetry samples, protected from fire by their low thermal conductivities, appeared unchanged after burning (Figure 9).

Another parameter for evaluating the fire behavior is FIGRA, which is defined by the ratio of PHRR to the time at which PHRR has been reached. This coefficient contains information on both the effect of time and heat release in a fire, providing information on flame spreading rate, the scale of a fire, and the flammability of the material. The FIGRA of P5C5-0 was measured at 9.3 W/s, which decreased to 6.9 W/s of P5C5-30, then to 4.9 W/s of P2C8-30, and finally to an extremely low value of 0.7 W/s of P1C9-30, indicating that the strengthened PVOH/clay aerogels have very low tendency to burn with high concentration of clay.

Figure 10 shows total smoke release (TSR) as a function of burning time. It can be seen that the smoke emitted during polymer combustion is significantly decreased with increasing clay content, from 182.3 for P5C5-30 to 25.5 for P2C8-30 and then to 15.0 m^2/m^2 for P1C9-30, consistent with the SEA values in Table 3. Smoke can represent a greater danger than fire itself, leading to rapid suffocation; the low levels of smoke

release from these aerogels supports their potential utility for consumer goods design.

The volatile products during burning are illustrated in Figure 11. The CO and CO_2 release seems related to the clay content. It is obvious that both gas products decrease significantly with increasing clay content. Another phenomenon observed is the decreases in CO and especially in CO_2 production with cross-

16232

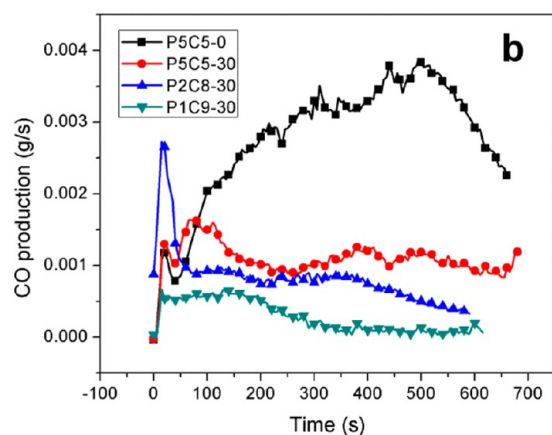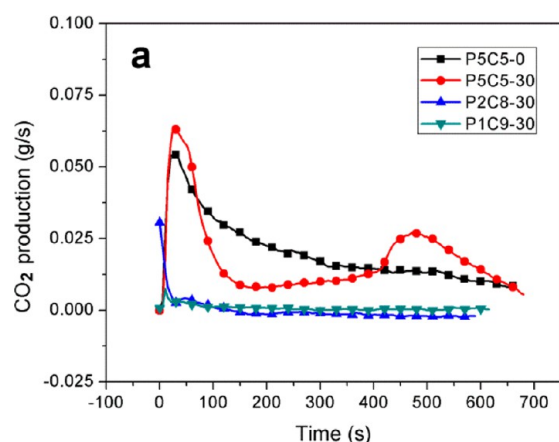dx.doi.org/10.1021/am504418w | ACS Appl. Mater. Interfaces 2014, 6, 16227−16236

Figure 11. Release rates of main volatile products of PVOH/clay aerogel as a function of burning time: a. carbon dioxide, b. carbon monoxide.

linking of the polymer. The mass loss of the samples as a function of burning time is illustrated in Figure 12. The weight loss occurs almost immediately once ignited, with a rate which appears to be proportional with the polymer content. The theoretical weight residue from burning would be expected to be similar to that of the clay content; this estimate was found to be low, and greater than expected quantities of residues
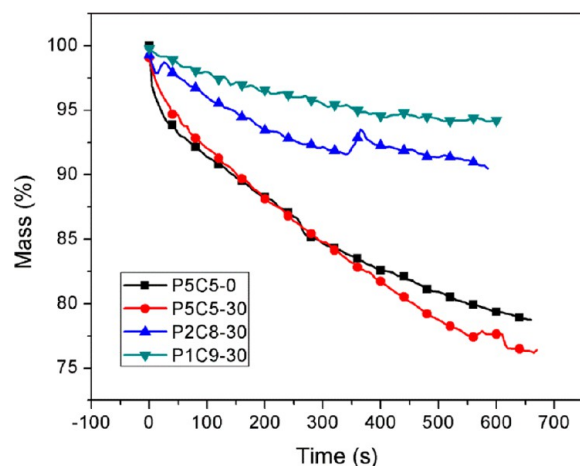

Figure 12. Mass loss of PVOH/clay aerogels as a function of burning time.

remained. For the P5C5 aerogel, for example, 75 wt % residue remained after combustion, compared with its 50 wt % of the theoretical value. The mass loss rates are in accord with the photos of the residues (Figure 9), which shows the samples were not burned completely. The top layer (fire side) of the sample turns black with char residue, while the bottom stays visibly unchanged. The results obtained with P2C8-30 and P1C9-30 were even more striking, quite different from most polymer samples, which generally leave little char residue unless they are highly flame retarded.[47−50]

Mechanism of Flammability Reduction. FTIR was used to examine the residues in different sample positions (Figure 13). The spectra show decreased organic content (characteristic
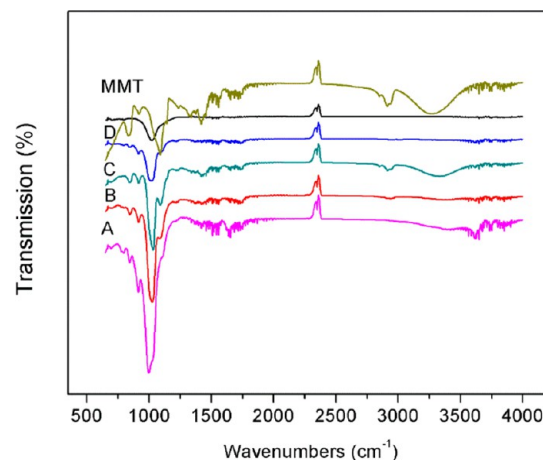

Figure 13. FTIR spectra of A, B, C, and D, stands for P5C5-30, the residue of P5C5-30 in the bottom, middle, and top layer of the sample, respectively. The FTIR spectrum of MMT is also listed as control.

peak: 1000 cm^{-1}, which corresponds to the C−O band) and confirmed the inhomogeneous and incomplete decomposition of the samples. WAXD was carried out to investigate the MMT clay within the aerogel composites (Figure 14). The clay showed a diffraction peak with 2θ at 7° (corresponds to the *d*-spacing of MMT clay),[51−53] which slightly decreased to 5° when incorporated into polymer, suggesting the existence of exfoliated inorganic layers throughout the polymer matrix.[54] The characteristic diffraction peak almost disappeared after burning, indicating a structural change for MMT clay. The
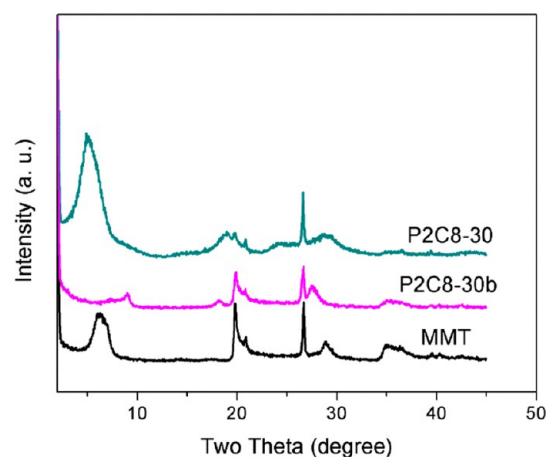

Figure 14. WAXD patterns of MMT clay, P2C8-30, and P2C8-30b.

photos and SEM results of the present study show that aerogel composite structures remain mostly intact after burning, even though the initial MMT structural features are lost (Figure 15). This structure information suggests that the materials may retain their useful properties, such as low thermal conductivity which results from porous structures.
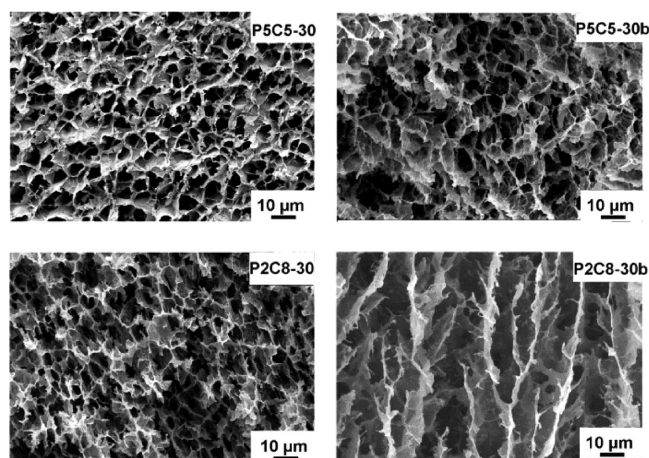

Figure 15. SEM micrographs of PVOH/clay aerogels and burnt residues.

It is intriguing to determine why the bottom of the sample was well protected from the effects of a large fire within the calorimeter. The bottom temperatures of the samples were monitored when burning in a cone calorimeter, with the results shown in Figure 16. Except for P5C5-0, which cracked and
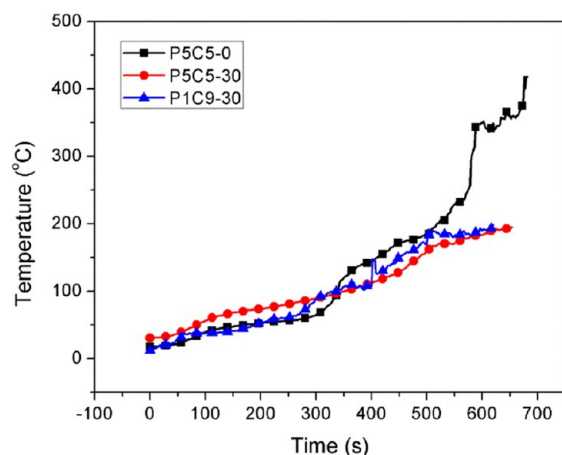

Figure 16. Temperature change of the sample bottom in cone calorimeter tests.

registered an increase in bottom temperature to 450 °C, the temperatures of aerogel samples (P5C5-30 and P1C9-30) increased only to 150 °C, less than the decomposition temperature of polymer, which therefore protected the underneath of the aerogels from degradation.

Cone calorimetry tests show that irradiation-cross-linked PVOH/clay aerogels possess inherently low flammabilities, with their heat releases attributed primarily to their polymer content. The heat release, smoke release, and volatile effluents of the four compositions tested all decrease significantly with increasing clay concentrations, leaving residue with little changes in dimensions after burning. Cross-linking of the

polymer further lowered the aerogel flammability, likely because of decreased chain mobility and increased difficulty in decomposing the network chain structure to combustible gas products. The reduction of flammability was especially pronounced for P1C9-30, which exhibited no open burning and extremely low production of gaseous reaction products. The following mechanisms can be proposed to explain the flammability results of this study:

(1) Fuel content decreases with increasing clay concentration. Silicate clays are noncombustible, hence with fixed total mass, increasing weight fractions of clay would naturally lead to decreased total release of heat, smoke, and other decomposition products, the main contributors to flammability. (2) MMT clay, itself, is a good heat insulation material with thermal conductivity as low as 0.03 W/mK, making it promising in many applications;[55] clay provides heat and mass transport barriers and therefore further reduces flammability. With its large surface/volume ratio, clay provides tortuous pathways for the oxygen and volatile decomposition products within the aerogel structure during combustion. Once ignited, it takes a longer time for the polymer underneath to decompose, and then the volatile effluents come out of the polymer matrix, thus decreasing the burning rate and the peak of heat release rate and suppressing the smoke and volatile effluents with increasing clay concentration. (3) The low thermal conductivity of the polymer/clay aerogels protects the polymer underneath (side opposite of the ignition source) from decomposing. The porous nature of the material endows it with very low thermal conductivity,[56] which combined with a high concentration of noncombustible clay in the aerogel maintains its structure largely unchanged during a fire.

4. CONCLUSIONS

Chemical-free fabrication of strengthened poly(vinyl alcohol) (PVOH)/clay aerogel composites via gamma irradiation was demonstrated, using water as solvent and an environmentally friendly freeze-drying process. The irradiated aerogels exhibit significantly increased compressive moduli compared to control materials, similar to those of rigid PU foams. Thirty kGy was found to be the optimum absorbed dose for fabricating strong PVOH composite for most samples. The microstructure of the aerogels becomes denser with increasing absorbed dose and PVOH content. TGA testing surprisingly shows that thermal stability of the aerogels decreases slightly with increasing irradiation doses, probably due to radiolysis of PVOH, but increases with increasing clay content. Cone calorimetry testing indicates that strengthened PVOH/clay aerogels possess extremely low flammabilities, due to the low PVOH content (fuel content) coupled with irradiation-induced cross-linking (chain mobility). The proposed mechanism is that the inherent inflammability of the clay filler, the tortuous path for combustion gases within the aerogel, and the low thermal conductivity of these materials all combine to produce the low flammability observed. Such low flammability aerogels with good mechanical properties are promising materials for both structural and consumer uses.

■ AUTHOR INFORMATION

Corresponding Authors
*E-mail: hongbing86@gmail.com (H.-B.C.).
*E-mail: das44@case.edu (D.A.S.).

■ REFERENCES

(1) Mackenzie, R. C. Clay-water Relationships. *Nature* **1953**, *171*, 681−683.

(2) Call, F. Preparation of Dry lay-gels by Freeze-drying. *Nature* **1953**, *172*, 126.

(3) van Olphen, H. Polyelectrolyte Reinforced Aerogels of Clays-application as Chromatographic Adsorbents. *Clay Miner.* **1967**, *15*, 423−435.

(4) Nakazawa, H.; Yamada, H.; Fujita, T.; Ito, Y. Texture Control of Clay-aerogel Through the Crystallization Process of Ice. *Clay Sci.* **1987**, *6*, 269−276.

(5) Wang, Y. X.; Gawryla, M. D.; Schiraldi, D. A. Effects of Freezing Conditions on the Morphology and Mechanical Properties of Clay and Polymer/clay Aerogels. *J. Appl. Polym. Sci.* **2013**, *129*, 1637−1641.

(6) Chen, H. B.; Chiou, B. S.; Wang, Y. Z.; Schiraldi, D. A. Biodegradable Pectin/clay Aerogels. *ACS Appl. Mater. Interfaces* **2013**, *5*, 1715−1721.

(7) Chiellini, E.; Corti, A.; D'Antone, S.; Solaro, R. Biodegradation of Poly(vinyl alcohol) Based Materials. *Prog. Polym. Sci.* **2003**, *28*, 963−1014.

(8) Hernandez, R.; Sarafian, A.; López, D.; Mijangos, C. Viscoelastic Properties of Poly(vinyl alcohol) Hydrogels and Ferrogels obtained through Freezing-thawing Cycles. *Polymer* **2004**, *46*, 5543−5549.

(9) Ricciardi, R.; Auriemma, F.; De Rosa, C. Structure and Properties of Poly(vinyl alcohol) Hydrogels obtained by Freeze/thaw Techniques. *Macromol. Symp.* **2005**, *222*, 49−63.

(10) Ricciardi, R.; D'Errico, G.; Auriemma, F.; Ducouret, G.; Tedeschi, A. M.; De Rosa, C.; Laupretre, F.; Lafuma, F. Short Time Dynamics of Solvent Molecules and Supramolecular Organization of Poly(vinyl alcohol) Hydrogels obtained by Freeze/thaw Techniques. *Macromolecules* **2005**, *38*, 6629−6639.

(11) Ricciardi, R.; Mangiapia, G.; Lo Celso, F.; Paduano, L.; Triolo, R.; Auriemma, F.; De Rosa, C.; Laupretre, F. Structure Organization of Poly(vinyl alcohol) Hydrogels obtained by Freezing and Thawing Techniques: a SANS Study. *Chem. Mater.* **2005**, *17*, 1183−1189.

(12) Ricciardi, R.; Auriemma, F.; Gaillet, C.; De Rosa, C.; Laupretre, F. Investigation of the Crystallinity of Freeze/thaw Poly(vinyl alcohol) Hydrogels by Different Techniques. *Macromolecules* **2004**, *37*, 9510−9516.

(13) Stauffer, S. R.; Peppas, N. A. Poly(vinyl alcohol) Hydrogels Prepared by Freezing-thawing Cyclic Processing. *Polymer* **1992**, *33*, 3932−3936.

(14) Yokoyama, F.; Masada, I.; Shimamura, K.; Ikawa, T.; Monobe, K. Morphology and Structure of Highly Elastic Poly(vinyl alcohol) Hydrogel Prepared by Repeated Freezing-and-Melting. *Colloid Polym. Sci.* **1986**, *264*, 595−601.

(15) Gupta, S.; Pramanik, A. K.; Kailath, A.; Mishra, T.; Guha, A.; Nayar, S.; Sinha, A. Composition Dependent Structural Modulations in Transparent Poly(vinyl alcohol) Hydrogels. *Colloids Surf., B* **2009**, *74*, 186−190.

(16) Immelman, E.; Sanderson, R. D.; Jacobs, E. P.; Van Reenen, A. J. Poly(vinyl alcohol) Gel Sublayers for Reverse Osmosis Membranes. I. Insolubilization by Acid-catalyzed Dehydration. *J. Appl. Polym. Sci.* **1993**, *50*, 1013−1034.

(17) Sanderson, R. D.; Immelman, E.; Bezuidenhout, D.; Jacobs, E. P.; van Reenen, A. J. Polyvinyl alcohol and Modified Polyvinyl Alcohol Reverse Osmosis Membranes. *Desalination* **1993**, *90*, 15−29.

(18) Immelman, E.; Bezuidenhout, D.; Sanderson, R. D.; Jacobs, E. P.; Van Reenen, A. J. Poly(vinyl alcohol) Gel Sub-layers for Reverse Osmosis membranes. III. Insolubilsation by Crosslinking with Potassium Peroxydisulphate. *Desalination* **1993**, *94*, 115−132.

(19) Gohil, J. M.; Bhattacharya, A.; Ray, P. Studies on the Cross-linking of Poly(vinyl alcohol). *J. Polym. Res.* **2005**, *13*, 161−169.

(20) Zhao, D. C.; Liao, G. Z.; Gao, G.; Liu, F. Q. Influences of Intramolecular Cyclization on Structure and Cross-linking Reaction Processes of PVA Hydrogels. *Macromolecules* **2006**, *39*, 1160−1164.

(21) Wang, Y. H.; Hsieh, Y. L. Crosslinking of Polyvinyl Alcohol (PVA) Fibrous Membranes with Glutaraldehyde and PEG Diacyl-chloride. *J. Appl. Polym. Sci.* **2010**, *116*, 3249−3255.

(22) Uragami, T.; Okazaki, K.; Matsugi, H.; Miyata, T. Structure and Permeation Characteristics of an Aqueous Ethanol Solution of Organic−Inorganic Hybrid Membranes Composed of Poly(vinyl alcohol) and Tetraethoxysilane. *Macromolecules* **2002**, *35*, 9156−9163.

(23) Zhang, Y.; Zhu, P. C.; Edgren, D. Crosslinking Reaction of Poly(vinyl alcohol) with Glyoxal. *J. Polym. Res.* **2010**, *17*, 725−730.

(24) Ito, Y.; Hasuda, H.; Yamauchi, T.; Komatsu, N.; Ikebuchi, K. Immobilization of Erythropoietin to Culture Erythropoietin-dependent Human Leukemia Cell Line. *Biomaterials* **2004**, *25*, 2293−2298.

(25) Muhlebach, A.; Muller, B.; Pharisa, C.; Hofmann, M.; Seiferling, B.; Guerry, D. New Water-soluble Photo Crosslinkable Polymers based on Modified Poly(vinyl alcohol). *J. Polym. Sci., Polym. Chem.* **1997**, *35*, 3603−3611.

(26) Nho, Y. C.; Park, K. R. Preparation and Properties of PVA/PVP Hydrogels Containing Chitosan by Radiation. *J. Appl. Polym. Sci.* **2002**, *85*, 1787−1794.

(27) Nuttelman, C. R.; Henry, S. M.; Anseth, K. S. Synthesis and Characterization of Photocrosslinkable, Degradable Poly(vinyl alcohol)-based Tissue Engineering Scaffolds. *Biomaterials* **2002**, *23*, 3617−3626.

(28) Wu, K. Y. A.; Wisecarver, K. D. Cell Immobilization using PVA Crosslinked with Boric Acid. *Biotechnol. Bioeng.* **1992**, *39*, 447−449.

(29) Alhassan, S. M.; Qutubuddin, S.; Schiraldi, D. A. Influence of Electrolyte and Polymer Loadings on Mechanical Properties of Clay Aerogels. *Langmuir* **2010**, *26*, 12198−12202.

(30) Gawryla, M. D.; Schiraldi, D. A. Novel Absorbent Materials Created via Ice Templating. *Macromol. Mater. Eng.* **2009**, *294*, 570−574.

(31) Wang, D. L.; Liu, Y.; Wang, D. Y.; Zhao, C. X.; Mou, Y. R.; Wang, Y. Z. A Novel Intumescent Flame-retardant System Containing Metal Chelates for Polyvinyl alcohol. *Polym. Degrad. Stab.* **2007**, *92*, 1555−1564.

(32) ZHao, C. X.; Liu, Y.; Wang, D. Y.; Wang, D. L.; Wang, Y. Z. Synergistic Effect of Ammonium Polyphosphate and Layered Double Hydroxide on Flame Retardant Properties of Poly(vinyl alcohol). *Polym. Degrad. Stab.* **2008**, *93*, 1323−1331.

(33) Pojanavaraphan, T.; Liu, L.; Ceylan, D.; Okay, O.; Magaraphan, R.; Schiraldi, D. A. Solution Cross-Linked Natural Rubber (NR)/Clay Aerogel Composites. *Macromolecules* **2011**, *44*, 923−931.

(34) Chen, H. B.; Hollinger, E.; Wang, Y. Z.; Schiraldi, D. A. Facile Fabrication of Poly(vinyl alcohol) Gels and Derivative Aerogels. *Polymer* **2014**, *55*, 380−384.

(35) Yoshii, F.; Zhanshan, Y.; Isobe, K.; Shinozaki, K.; Makuuchi, K. Electron Beam Crosslinked PEO and PEO/PVA Hydrogels for Wound Dressing. *Radiat. Phys. Chem.* **1999**, *55*, 133−138.

(36) Nagasawa, N.; Yagi, T.; Kume, T.; Yoshii, F. Radiation Crosslinking of Carboxymethyl Starch. *Carbohydr. Polym.* **2004**, *58*, 109−113.

(37) Razzak, M. T.; Erizal, Z.; Dewi, S. P.; Lely, H.; Sukirno, T. E. The characterization of Dressing Component Materials and Radiation Formation of PVA−PVP Hydrogel. *Radiat. Phys. Chem.* **1999**, *55*, 153−165.

(38) Zhao, L.; Xu, L.; Mitomo, H.; Yoshii, F. Synthesis of pH-sensitive PVP/CM-chitosan Hydrogels with Improved Surface Property by Irradiation. *Carbohydr. Polym.* **2006**, *64*, 473−480.

(39) Gawryla, M. D.; van den Berg, O.; Weder, C.; Schiraldi, D. A. Clay Aerogel/cellulose Whisker Nanocomposites: a Nanoscale Wattle and Daub. *J. Mater. Chem.* **2009**, *19*, 2118−2124.

(40) Johnson, J. R.; Schiraldi, D. A.; Spikowski, J. Mineralization of Polymer/clay aerogels: A Bioinspired Approach to Composite Reinforcement. *ACS Appl. Mater. Interfaces* **2008**, *1*, 1305−1309.

(41) Chen, H. B.; Wang, Y. Z.; Sanchez-Soto, M.; Schiraldi, D. A. Low flammability, Foam-like Materials Based on Ammonium Alginate and Sodium Montmorillonite Clay. *Polymer* **2012**, *53*, 5825−5831.

(42) Danno, A. Gel Formation of Aqueous Solution of Polyvinyl Alcohol Irradiated by Gamma Rays from Cobalt-60. *J. Phys. Soc. Jpn.* **1958**, *13*, 722−727.

(43) Yang, S. L.; Wu, Z. H.; Yang, W.; Yang, M. B. Thermal and Mechanical Properties of Chemical Crosslinked Polylactide (PLA). *Polym. Test.* **2008**, *27*, 957−963.

(44) Levchik, G. F.; Si, K.; Levchik, S. V.; Camino, G.; Wilkie, C. A. The Correlation Between Cross-linking and Thermal Stability: Cross-linked Polystyrenes and Polymethacrylates. *Polym. Degrad. Stab.* **1999**, *65*, 395−403.

(45) Zanetti, M. Flammability and Thermal Stability of Polymer/layered Silicate Nanocomposites. In *Polymer Nanocomposites*; Mai, Y. W., Yu, Z. Z., Eds.; Woodhead, Cambridge: Cambridge, UK, 2006; pp 256−72.

(46) Laoutid, F.; Bonnaud, L.; Alexandre, M.; Lopez-Cuesta, J.-M.; Dubois, P. New Prospects in Flame Retardant Polymer Materials: From Fundamentals to Nanocomposites. *Mater. Sci. Eng. R* **2009**, *63*, 100−125.

(47) Chen, H. B.; Zhang, Y.; Chen, L.; Shao, Z. B.; Liu, Y.; Wang, Y. Z. Novel Inherently Flame-Retardant Poly(trimethylene Terephthalate) Copolyester with the Phosphorus-Containing Linking Pendent Group. *Ind. Eng. Chem. Res.* **2010**, *49*, 7052−7059.

(48) Zhao, B.; Chen, L.; Long, J. W.; Chen, H. B.; Wang, Y. Z. Aluminum Hypophosphite versus Alkyl-Substituted Phosphinate in Polyamide 6: Flame Retardance, Thermal Degradation, and Pyrolysis Behavior. *Ind. Eng. Chem. Res.* **2013**, *52*, 2875−2886.

(49) Wang, D. Y.; Liu, Y.; Wang, Y. Z.; Artiles, C. P.; Hull, T. R.; Price, D. Fire Retardancy of a Reactively Extruded Intumescent Flame Retardant Polyethylene System Enhanced by Metal Chelates. *Polym. Degrad. Stab.* **2007**, *92*, 1592−1598.

(50) Wang, D. Y.; Liu, Y.; Ge, X. G.; Wang, Y. Z.; Stec, A.; Biswas, B.; Hull, T. R.; Price, D. Effect of Metal Chelates on the Ignition and Early Flaming Behaviour of Intumescent Fire-Retarded Polyethylene systems. *Polym. Degrad. Stab.* **2008**, *93*, 1024−1030.

(51) Vassiliou, A. A.; Chrissafis, K.; Bikiaris, D. N. In situ prepared PET nanocomposites: Effect of Organically Modified Montmorillonite and Fumed Silica Nanoparticles on PET Physical Properties and Thermal Degradation Kinetics. *Thermochim. Acta* **2010**, *500*, 21−29.

(52) Chang, J. H.; Kim, S. J.; Joo, Y. L.; Im, S. Poly(ethylene terephthalate) Nanocomposites by in situ Interlayer Polymerization: the Thermo-mechanical Properties and Morphology of the Hybrid Fibers. *Polymer* **2004**, *45*, 919−926.

(53) Chang, J. H.; An, Y. U. Nanocompositesof Polyurethane with Various Organo clays: Thermomechanical Properties, Morphology, and Gas Permeability. *J. Polym. Sci., Polym. Phys. Ed.* **2002**, *40*, 670−677.

(54) Strawhecker, K. E.; Manias, E. Structure and Properties of Poly(vinyl alcohol)/Na+ Montmorillonite Nanocomposites. *Chem. Mater.* **2000**, *12*, 2943−2949.

(55) Wang, X. Y.; Zhong, J. M.; Wang, Y. M.; Yu, M. F. A Study of the Properties of Carbon Foam Reinforced by Clay. *Carbon* **2006**, *44*, 1560−1564.

(56) Hostler, S. R.; Abramson, A. R.; Gawryla, M. D.; Bandi, S. A.; Schiraldi, D. A. Thermal Conductivity of a Clay-based Aerogel. *Int. J. Heat Mass Transfer* **2009**, *52*, 665−669.